International Journal of Nanoelectronics and Materials
IJNeaM
ISSN 1985-5761 | E-ISSN 2232-1535

Comparative evaluation of CTAB and AP1 buffers in on-chip DNA extraction of pathogenic fungus for microfluidic interdigitated-electrode biosensing.

Adilah Ayoib [a,b,c] *, Shahidah Arina Shamsuddin [b,d], Nor Azizah Parmin [b], Rajapaksha Dewage Asanka Amith Rajapaksha [e]

[a]*Faculty of Chemical Engineering & Technology, Universiti Malaysia Perlis (UniMAP), Arau 02600, Malaysia*
[b]*Institute of Nano Electronic Engineering, Universiti Malaysia Perlis (UniMAP), Kangar 01000, Malaysia*
[c]*Carbon Sustainability Nexus (CaSNex), Special Interest Group (SIG), Universiti Malaysia Perlis (UniMAP), Arau 02600, Malaysia*
[d]*Faculty of Mechanical Engineering & Technology, Universiti Malaysia Perlis (UniMAP), Padang Besar 02100, Malaysia*
[e]*Department of Nano Science Technology, Faculty of Technology, Wayamba University of Sri Lanka, Kuliyapitiya 60200, Sri Lanka*
** Corresponding author. Tel.: +6013-509-2811; e-mail: adilahayoib@unimap.edu.my*

Received XXX 2023, Revised XXX 2023, Accepted XXX 2023

ABSTRACT

Conventional methods such as tissue culture and PCR based analyses are expensive, time-consuming, often requiring up to two weeks and intensive labor. In contrast, microfluidic lab-on-a-chip systems enable rapid (1 hour) detection with lower cost and minimal sample volume. This study outlines a streamlined PDMS microfluidic workflow for on-chip DNA extraction and label-free detection of *Ganoderma boninense,* the pathogenic fungus that has been identified to be the major pathogen for palm oil plantation in several countries, especially in Malaysia. Two lysis buffers, cetyltrimethylammonium bromide (CTAB) and AP1, were compared for DNA yield and purity. UV–Vis analysis showed that AP1 consistently produced higher DNA concentrations, whereas CTAB extracts had smoother absorbance spectra (indicating fewer impurities). All extracts exhibited the expected peak near 260 nm, with shoulders around 280–290 nm, where both dsDNA and ssDNA can be found, indicating successful DNA extraction on microfluidics chip. Electrical I–V measurements on the AuNP–ZnO–coated interdigitated-electrode (IDE) biosensor demonstrated increased DNA hybridization signal, confirming successful extraction and detection. These results indicate that AP1 yields higher DNA recovery (with more background absorbance) while CTAB yields cleaner DNA. Our integrated microfluidic system enables fast, sensitive detection of *G. boninense*, highlighting its potential for field-deployable diagnostics.

Keywords: *DNA extraction, PDMS, Microfluidics, Biosensor, Lab-on-a-chip*

1. INTRODUCTION

Ganoderma boninense is a soil-borne fungal pathogen that causes basal stem rot (BSR), the most serious disease of oil palm in Malaysia and neighboring countries [1]. BSR can infect young palms asymptomatically and leads to devastating yield losses, underscoring the need for early detection. Conventional diagnostics, such as tissue culture and polymerase chain reaction (PCR) are expensive and time-consuming, often taking weeks to yield results. In contrast, microfluidic lab-on-a-chip (LOC) biosensors integrate sample preparation and detection, enabling faster, lower-cost analysis from small samples [2], [3], [4]. Table 1 summarizes recent microfluidic DNA extraction and detection platforms across a range of pathogens and sample types. In comparison, our platform integrates on-chip chemical lysis and DNA extraction with label-free electrical hybridization detection, achieving a simplified and expedited single-step workflow of approximately 1 hour. It eliminates the need for magnetic beads and amplification, while minimizing reagent use, thereby speeding overall assay time relative to existing systems.

In this study, we developed a single-channel polydimethylsiloxane (PDMS) microfluidic chip for on-chip utilizing an interdigitated-electrode (IDE) biosensor. We compared two lysis chemistries: cetyltrimethyl-ammonium bromide (CTAB) and AP1 buffer (QIAGEN®, Germany), contrasting traditional fungal lysis, which is effective at removing polysaccharides and phenolics (CTAB), with the commercial AP1 buffer that incorporates polyvinylpyrrolidone/dithiothreitol (PVP/DTT) to improve yield in polyphenolic fungal matrices. This trade-off between purity (CTAB) and recovery (AP1) is central to our comparative evaluation, as we aim to determine which method yields higher DNA recovery and better sensor response. Finding a suitable lysis buffer for on-chip DNA extraction is essential to achieving optimal outcomes.

This proof-of-concept (Figure 1) integrates microfluidic engineering with molecular diagnostics, paving the way for rapid *G. boninense* detection in agricultural settings. The outcomes of this study could significantly enhance disease management strategies and contribute to sustainable oil palm cultivation.

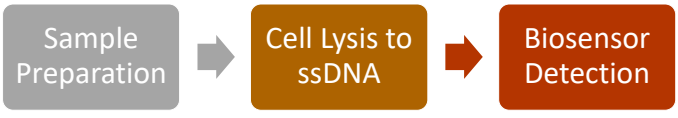

Figure 1. Overview of DNA extraction on a LOC system.

Table 1. Advances in Microfluidic DNA Extraction and Detection Over the Past Decade

No.	Microfluidic System	Extraction Method	Key Results	Ref.
1.	Thermally-actuated IFAST chip (stool interface)	Chaotropic lysis + dried magnetic particles (PMPs)	Rapid DNA release and binding in 7 min from crude stool; 40× volume concentration; platform for POC DNA prep	[5]
2.	Automated chip with magnet-actuation (environmental samples)	Thermal/chemical/enzymatic cell lysis + magnetic-particle purification	LOD ≈10^2–10^3 genome/mL in water, 1–10 GE/10L in air; detected Campylobacter DNA in farm air samples	[6]
3.	Integrated PCR/LAMP lab-on-chip (Fraunhofer prototype)	On-chip cell lysis (with optional magnetic bead DNA extraction)	Proof-of-concept multiplex pathogen test: on-chip bacterial isolation, lysis, DNA extraction, amplification (LAMP/PCR) for *E. coli* and *Salmonella* detection	[7]
4.	Polymer/paper "IPμchip" platform (portable)	On-chip magnetic-bead DNA extraction	15 min extraction vs >90 min manual; LAMP amplification of *S. pneumoniae/M. pneumoniae* to 20 fg sensitivity; smartphone readout, point-of-care multiplex detection	[8]
5.	Finger-actuated microfluidic biosensor (Anal. Chem.)	Immuno-magnetic capture + silica-coated MNP DNA absorption	"Sample-in-answer-out" *E. coli* O157:H7 assay; RPA-CRISPR/Cas12a detection, LOD 10 CFU/mL, range 10^2–10^8 CFU/mL in 2.5 h; recovery 104–120%	[9]
6.	PDMS-based microfluidic chip fabricated using SU-8 photoresist on glass substrate	Automated, high-throughput DNA extraction protocol integrated with a label-free biosensor	Achieved DNA extraction and detection of *G. boninense* within 2 hours; UV–Vis, FTIR, and PCR confirmed effectiveness; device showed ≤0.1 mm fabrication tolerance	[10]
7.	Portable lab-on-chip device utilizing magnetic beads	Modified on-chip DNA extraction methodology	Enabled DNA extraction of *G. boninens* in ~15 minutes; PCR validation showed comparable performance to benchtop protocols; system accommodated two samples of 120 µL	[11]
8.	Integrated microfluidic cfDNA chip (Anal. Chem.)	Vortex micromixer + magnetic beads with capture probes	76% cfDNA recovery (200 µL plasma) in 45 min; on-chip allele-specific qPCR for *BRCA1* mutations in 90 min; enables automated screening for cancer biomarkers	[12]
9.	Handheld capillary LAMP chip (Food Chem)	Microneedle DNA extraction (on-chip)	Colorimetric LAMP on chip for meat species authentication; pricking meat with microneedle releases DNA; 6 meat species distinguished; detection of 1% adulteration in 60 min; cost <$1 per test	[13]
10.	Rotating-cartridge POCT PCR platform (Sci. Rep.)	Integrated cartridge with lyophilized reagents (encapsulated extraction reagents)	Simultaneous 6-plex virus testing (HPV, SARS-CoV-2, etc.) in 1 h; LOD 1000 copies/mL for HPV, 200 copies/mL for SARS-CoV-2; 100% sensitivity, >98% specificity in clinical samples	[14]
11.	µPAD LAMP-CRISPR platform (NPJ Sci. Food)	Magnetic silica beads (tube extraction) + on-chip LAMP & CRISPR/Cas12a	Portable device (syringe & tubing) integrates magnetic bead DNA extraction with LAMP-CRISPR. Total assay ~1 h; detected *Salmonella* at 10^2 CFU/mL in food samples; visual readout via smartphone; high specificity	[15]
12.	Microfluidic qPCR array (Sci. Rep.)	Off-chip extraction, on-chip qPCR	Multiplex qPCR chip for 21 respiratory viruses from clinical swabs; detected ≥1 virus in 76.6% of samples (n=158), including rhinovirus, adenovirus, etc.; demonstrated high-throughput surveillance capability	[16]
13.	Integrated PMMA POCT chip (Microsyst. Nanoeng.)	Adsorption on magnetic nanoparticles	SARS-CoV-2 sample-to-answer: 5 min load, 3 min magnetic bead RNA extraction, 20 min RT-LAMP (total 28 min); LOD <297 copies; cost ≈$9.5 per test; performance comparable to benchtop kits	[17]
14.	Pressure-driven micro-chamber array (Lab Chip)	On-chip spheroplast lysis	Extraction of intact bacterial chromosomes: single *B. subtilis* genome isolated in microfluidic chamber (lysing in situ). DNA deproteinated on-chip; demonstrated genome release and addition of exogenous factors for genome-in-a-box studies	[18]
15.	Gravity-driven microcapillary siphon array (Lab Chip)	Magnetic bead (silica) DNA binding in capillaries	Bacterial DNA extraction from complex matrices (blood, water): using 10×200 µm capillaries and external magnet; achieved >90% recovery vs 52% manual; linear qPCR detection of *E. coli* in buffer, blood, river water; reusable chip with no cross-contamination	[19]
16.	Multiplex CRISPR microfluidic chip (Talanta)	Off-chip RPA amplification + on-chip CRISPR-Cas12a	"Space-coded" chip partitions RPA amplicons for 9 respiratory viruses (influenza A/B, 4 coronaviruses, RSV, etc.) in one run; detection <40 min; LOD ~1 copy/reaction (10^−18 M); tested on 35 patient samples: 90% sensitivity, 100% specificity	[20]

2. METHODOLOGY

2.1. Design and Fabrication of Microfluidic Chip

The microfluidic chip is fabricated using a two-stage process: first, a master template is created with SU-8, followed by the replication of PDMS on a microscope glass substrate for low-cost fabrication, as previously described in our papers [21], [22]. Briefly, an AutoCAD-designed photomask was printed on high-resolution transparency and used to pattern SU-8 photoresist on a glass substrate via photolithography. The resulting SU-8 master mold was coated with PDMS, cured, and peeled off. Inlet and outlet holes were punched into the PDMS, which was then plasma-bonded to a new glass slide to form sealed microfluidic channels. Figure 2 illustrates this process.

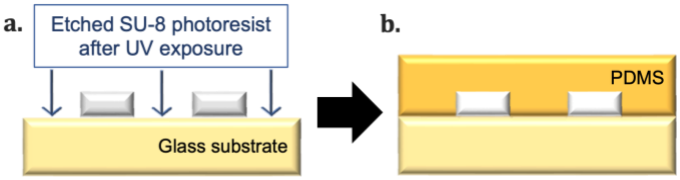

Figure 2. The two-stage fabrication of PDMS microfluidics. **a.** Development of SU-8 master template via photolithography process. **b.** Plasma bonding of PDMS replicate on glass substrate to create microfluidic channels after the soft lithography process.

2.2. Fungal Growth and Cultivation

G. boninense cultures were grown in potato dextrose broth (PDB) at room temperature (30°C ± 2) and 250 rpm for 12 days. A 0.5 mL aliquot was then transferred onto potato dextrose agar (PDA) plates and incubated for one additional week to generate fresh hyphae. These fungal mycelia were used for downstream DNA extraction Figure 3.

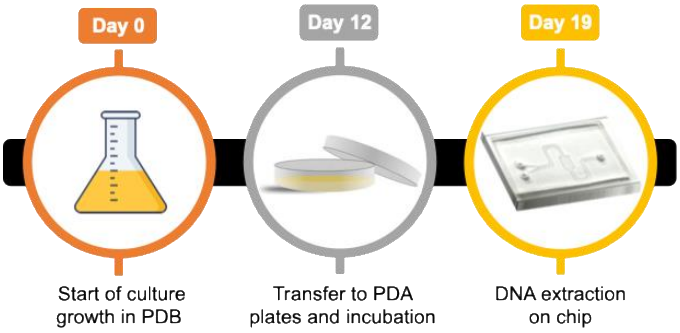

Figure 3. Schematic illustration of fungal cultivation for DNA extraction on a microfluidic chip.

2.3. Preparation of Lysis Buffers and DNA Extraction On-Chip

Two lysis buffers were prepared for on-chip extraction [10]: a CTAB-based buffer (100 mM Tris-HCl pH 8.4, 1.4 M NaCl, 25 mM EDTA, 2% CTAB) pre-heated to 65°C, and AP1 buffer (10 mM Tris-HCl pH 8.0, 1 mM EDTA, 0.1% SDS, 0.1 M NaCl, 1× PVP, 10 mM DTT) used at room temperature. Each buffer was supplemented immediately before use with 5 mg/mL proteinase K and 50 µg/mL RNase A. We infused these lysis solutions into the chip to lyse cells and release DNA. DNA extracts were collected from the outlet at three time points: immediately, 4 hours later, and after overnight incubation. Samples collected without added NaOH yielded double-stranded DNA (dsDNA), whereas adding NaOH produced single-stranded DNA (ssDNA). All samples and synthetic DNA controls were analyzed by UV–Vis spectrophotometry to assess DNA yield and purity.

2.4. Molecular and Electrical Characterization of DNA Using UV-Vis Spectroscopy and Functionalized Interdigitated Electrode Biosensor Measurements

The extracted DNA samples were analyzed by UV–Vis spectrophotometry (PerkinElmer) to quantify DNA concentration and assess purity based on the 260 nm absorbance peak. Electrical characterization was performed on a functionalized IDE biosensor designed and fabricated as previously described [23], [24].(Keithley 2200 SMU, USA). The IDE surface was coated with zinc oxide and gold nanoparticles (AuNPs) (30 nm) (Sigma Aldrich, USA) to enhance conductivity. A thiolated *G. boninense* ssDNA probe was immobilized on the AuNP-coated IDE, forming a specific recognition layer. Target DNA extracts were applied to the biosensor, and current-voltage (0–1 V) curves were recorded to detect hybridization. We compared I–V responses between devices with and without the AuNPs coating to evaluate the hybridization signal.

3. RESULTS AND DISCUSSION

3.1. PDMS Chip Morphology

After fabrication, the SU-8 master mold and PDMS channel were imaged under low power microscopy (S-EYE software) (Figure 3). Measured dimensions (Table 2) matched the design specifications. Assembly of the transparency print, master mold, and final PDMS chip is shown in Figure 4. Water flow tests showed no leakage, confirming the integrity of the plasma-sealed channel.

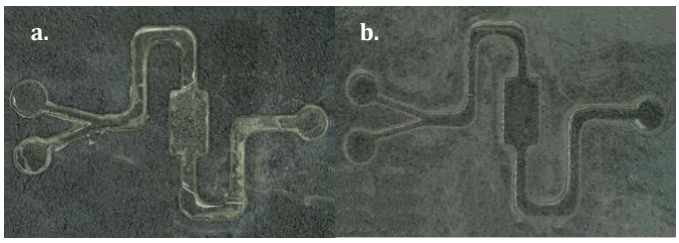

Figure 3. Images of the fabricated microfluidic chip under low power microscopy. **a.** SU-8 master template **b.** PDMS replicate

Table 2. Size and dimension of the microfluidic chip design on AutoCAD software

Design	Dimension (mm)
Inlet width	0.5
Inlet radius	1.4
Outlet width	1.0
Outlet radius	1.3
Cell-capture width × length	3.0 × 5.0

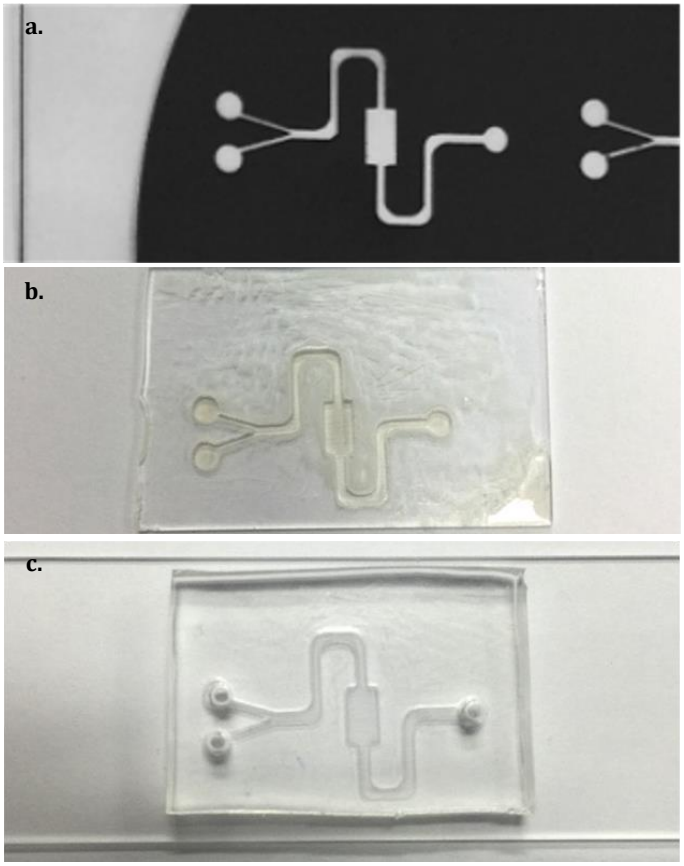

Figure 4. Images of the microfluidic chip at its initial and completed stages. **a.** Printed design of the microfluidic chip on transparency. **b.** Fabricated microfluidic SU-8 master template. **c.** Fully assembled microfluidic chip ready for DNA extraction.

3.2. UV-Vis Vis Analysis on CTAB and AP1 method of DNA Extraction on Microfluidic Chip

The UV-Vis spectra of DNA extracts, presented in Figures 5 and 6, illustrate the absorbance characteristics of samples collected from the outlet at various time intervals. Pure DNA is expected to exhibit a peak around 260 nm [3], [23], [24], [25], as evidenced by the synthetic control depicted in both figures. Conversely, absorbance levels of raw samples, used as negative controls, remain negligible. Both extraction methods confirmed the presence of DNA; however, the AP1 extracts (Figure 6) yielded a significantly higher concentration compared to the CTAB extracts (Figure 5), as indicated by elevated A260 absorbance values (Table 3).

Table 3. DNA concentration at different time

Sample	A260	A260/ A280	A260/ A230
Synthetic ssDNA	2.31	1.54	1.16
ssDNA CTAB immediately	1.39	1.70	0.14
ssDNA CTAB after 4 hours	2.23	1.84	0.54
ssDNA CTAB overnight	3.16	2.01	0.32
ssDNA AP1 immediately	3.03	1.47	0.97
ssDNA AP1 after 4 hours	3.54	1.81	0.35
ssDNA AP1 overnight	3.53	1.49	1.05

The enhanced performance of the AP1 extracts can be attributed to the inclusion of polyvinylpyrrolidone (PVP) in the AP1 buffer, which binds polyphenolic inhibitors through hydrogen bonding [26], thereby improving DNA recovery from crude fungal lysates. In contrast, CTAB extracts exhibit a smoother spectrum with lower baseline noise (Figure 5), indicating reduced interference from impurities. A shift in the absorbance peak imply the presence of additional molecules concomitant with the DNA, while a slight shoulder around 230 nm in both extracts might indicate residual salts or phenolic compounds, particularly in the CTAB extracts. Thus, while AP1 lysis yielded a greater quantity of DNA, CTAB lysis produced comparatively purer DNA.

The absorbance ratios A260/A280 and A260/A230 were analyzed as secondary indicators of DNA purity (Table 3). Conventionally, an A260/A280 ratio in the range of 1.7–1.9 suggests relatively pure DNA. Our analysis revealed that the synthetic ssDNA control exhibited an A260 of 2.3 with a A260/A280 ratio of 1.54. In comparison, AP1-extracted samples frequently exceeded 3.0 OD units at 260 nm, reflecting a highly concentrated DNA solution that may potentially exceed the spectrophotometer's linear detection range. In contrast, CTAB-extracted samples displayed lower A260 values and A260/A280 ratios of 1.7-2.0, potentially indicating lower levels of co-extracted organic contaminants or salts. Notably, the A260/A280 values for both AP1 and CTAB samples after 4 hours are 1.8, indicating the suitability of this time frame for DNA analysis.

It is well established that pH variations can significantly influence absorbance ratios [27], [28]. Acidic conditions typically reduce the A260/A280 ratio by 0.2–0.3 units, whereas alkaline conditions can elevate it similarly. Additionally, A260/A230 ratios, typically expected to fall between 2.0 and 2.2 for pure DNA, are sensitive to contaminants such as residual proteins, polysaccharides, phenolics, chaotropic salts, and buffer components. All measured A260/A230 ratios in this study fell below the conventional purity threshold. One plausible explanation is the use of deionized water as a spectrophotometric blank, while the sample DNA was suspended in Tris-EDTA (TE) buffer. Differences in ionic strength and pH between the blank and sample matrices likely contributed to absorbance shifts and artificially lowered purity ratios. Furthermore, residual NaOH from the ssDNA generation process may have introduced slight pH imbalances, distorting absorbance measurements.

The elevated A260 values observed in real DNA extracts, compared to the synthetic standard, suggest that other nucleic acid species, such as RNA or free nucleotides, may have contributed to the total absorbance. This observation aligns with the fact that the chip-based extraction protocol employed in this study did not include additional purification or cleanup steps beyond cell lysis, limiting its suitability for applications requiring high-purity DNA. It is important to note that the primary objective of this study was not to assess DNA purity but rather to establish a label-free detection methodology utilizing the biosensor chip. Therefore, the mere detection of DNA's presence is sufficient.

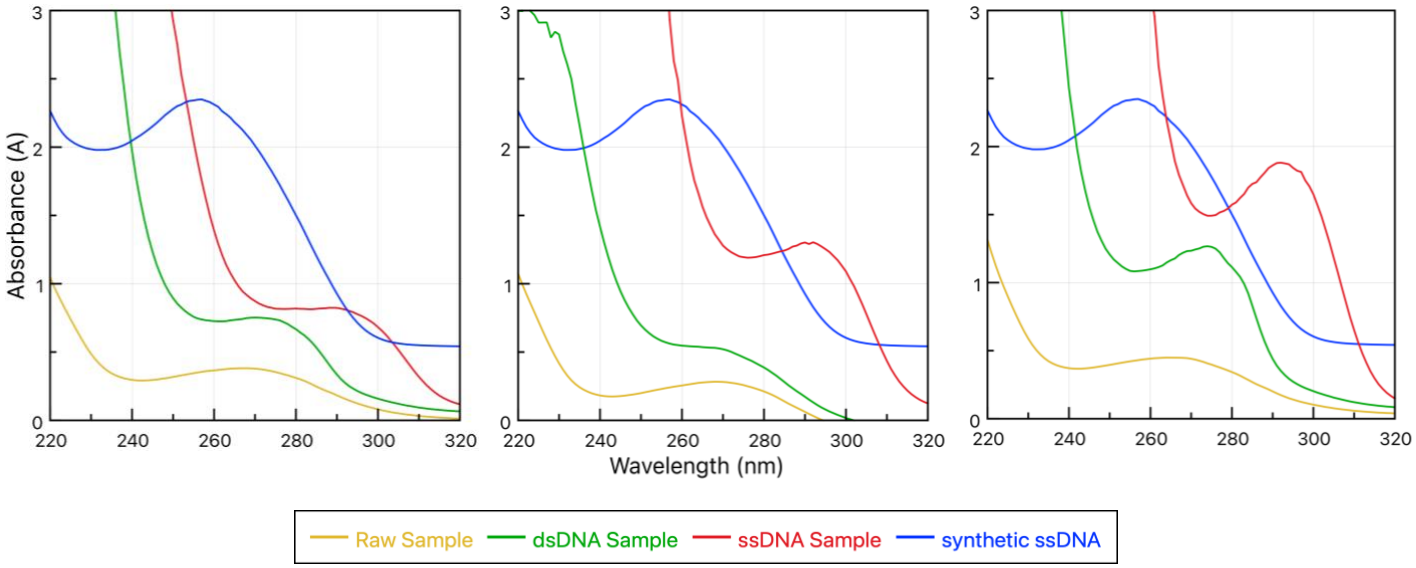

Figure 5. UV-Vis Spectroscopy *G. boninense* DNA extract using CTAB method at different time intervals. **a.** immediately; **b**. after 4 hours; **c.** overnight.

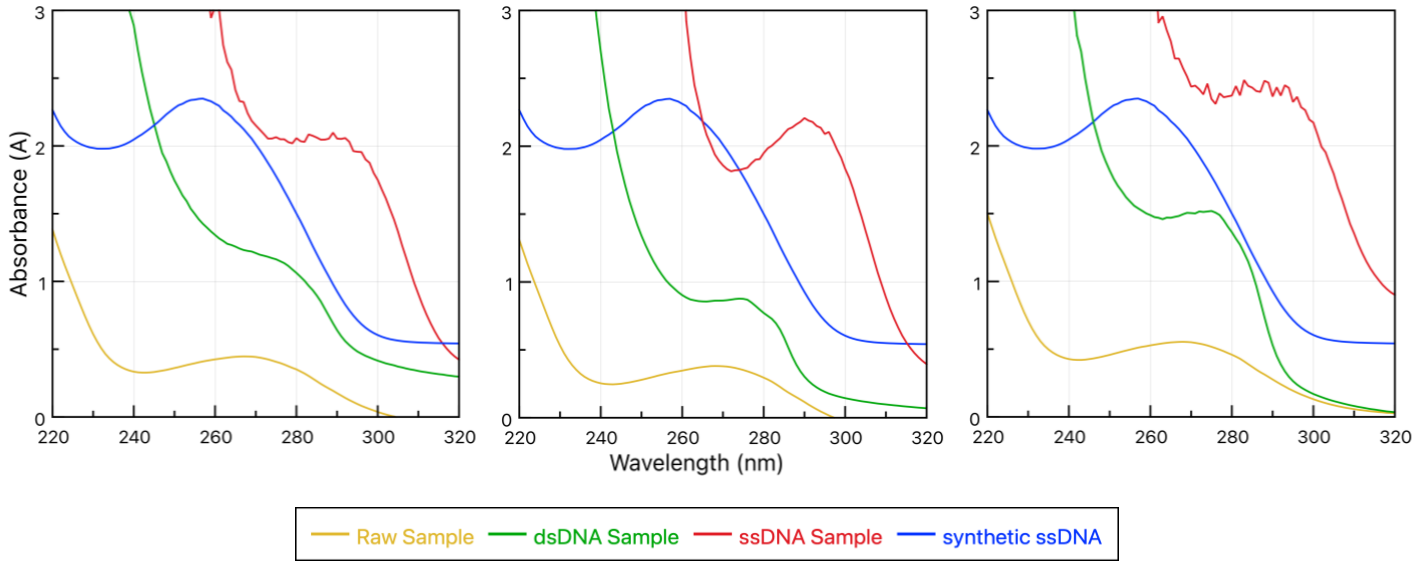

Figure 6. UV-Vis Spectroscopy *G. boninense* DNA extract using AP1 method at different time intervals. a**.** immediately; **b.** after 4 hours; **c.** overnight.

Additionally, spectral shoulders near 230 nm in both extraction methods may be attributed to buffer components such as EDTA or carbohydrate impurities commonly present in fungal samples. While CTAB-based methods efficiently precipitate DNA through high salt concentrations and detergent activity, they are also prone to co-extracting polysaccharides and phenolic compounds unless followed by purification steps. In contrast, the AP1 buffer, through the inclusion of PVP, appears more effective in mitigating such contamination, enhancing DNA yield. This distinction explains why AP1-derived extracts exhibited higher absorbance and concentration values, despite CTAB extracts appearing spectrally "cleaner."

Overall, our results align with the expectations of the chip-based extraction method employed for single-use detection applications, highlighting the efficacy of the AP1 method in generating DNA extracts suitable for subsequent experiments. Notably, DNA can be extracted within an hour.

3.3. DNA Detection on Functionalized Biosensor

Electrical characterization was carried out using current–voltage (I–V) measurements on the IDE biosensor to examine the current flow of microelectrodes and connectivity changes before and after the hybridization process. Based on Figures 7. and 8., the non-hybridized probes showed near-zero current (baseline). Immobilized probe DNA (negative control) in both figures show significantly higher than that for both real and synthetic ssDNA at 1.0 V, likely due to changes in resistance after immobilization.

In an IDE biosensor designed for DNA detection, the immobilization of the probe DNA and subsequent hybridization with the target DNA led to distinct changes in the electrochemical behavior of the system. During the immobilization process, probe ssDNA are covalently attached to the IDE surface, contributing to a modest increase in surface charge density and promoting ion conductivity in the sensing medium. This leads to a higher current as counterions freely diffuse to balance the negatively charged phosphate backbone of the probe ssDNA [29], maintaining high ionic mobility near the surface of the electrode.

Upon hybridization, complementary target DNA binds to the probe, forming dsDNA. This transition creates a "crowding effect," increasing the density of phosphate groups and further amplifying negative charge near the electrode-solution interface [30], [31]. However, the higher charge density impedes ionic mobility in the electrical double layer due to electrostatic repulsion and the bulkier dsDNA structure. As a result, the current often decreases after hybridization. Additionally, hybridization alters the dielectric properties of the interface, as the less flexible dsDNA obstructs ion diffusion and increases resistance. This combination of effects leads to a measurable reduction in current, which serves as the basis for signal detection in electrochemical biosensors.

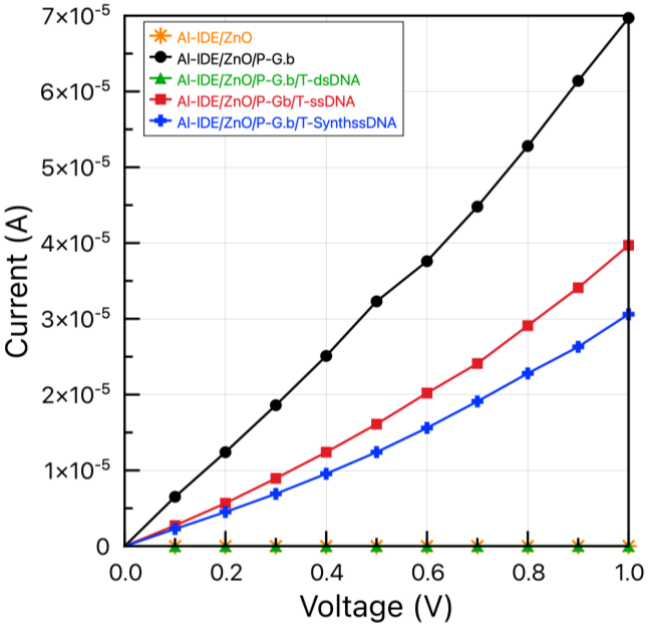

Figure 7. Electrical characterization of G. boninense DNA extract. without AuNPs coating. Al: Aluminum; IDE: Interdigitated Electrode; ZnO: Zinc oxide; AuNPs: Gold nanoparticles; P-G.b: Probe DNA immobilization of G. boninense; T-dsDNA: Target hybridization of dsDNA real sample (non-complementary); T-ssDNA: target hybridization of ssDNA real sample (complementary); T-SynthessDNA: target hybridization of synthetic ssDNA sample (complementary).

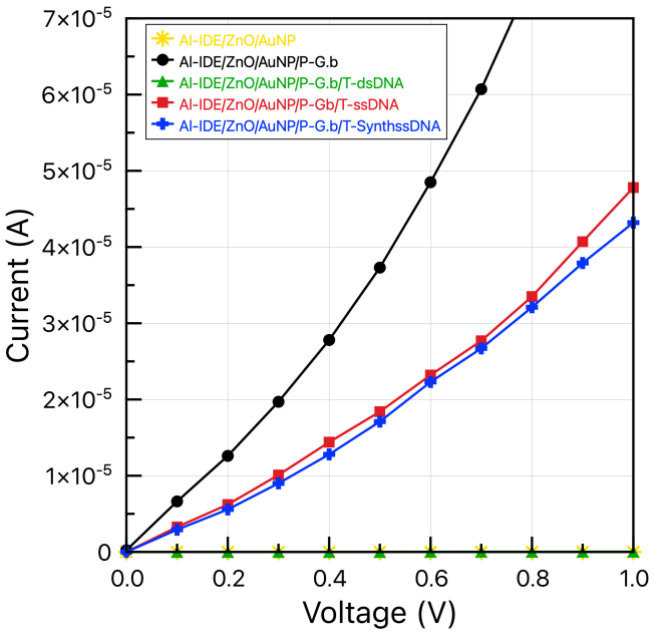

Figure 8. Electrical characterization of G. boninense DNA extract with AuNPs coating. Al: Aluminum; IDE: Interdigitated Electrode; ZnO: Zinc oxide; AuNPs: Gold nanoparticles; P-G.b: Probe DNA immobilization of G. boninense; T-dsDNA: Target hybridization of dsDNA real sample (non-complementary); T-ssDNA: target hybridization of ssDNA real sample (complementary); T-SynthessDNA: target hybridization of synthetic ssDNA sample (complementary).

The addition of complementary target DNA caused a substantial current increase in both AuNP-coated and non-AuNP-coated IDEs (Figure 7. Al-IDE/ZnO/P-G.b/T-ssDNA, and Figure 8. Al-IDE/ZnO/AuNP/P-G.b/T-ssDNA), confirming hybridization. Non-complementary control samples, Figure 7. Al-IDE/ZnO/P-G.b/T-dsDNA, and Figure 8. Al-IDE/ZnO/AuNP/P-G.b/T-dsDNA, showed current change nearly equivalent to zero, consistent with their roles as negative controls (no target to hybridize, hence no positive charge carriers). The real (higher-concentration) sample generated a larger current compared to the synthetic standard, consistent with more hybridization, though the values are lower than those observed for the immobilized probe DNA.

Additionally, the AuNP-coated IDE (Figure 8) consistently exhibited higher current responses compared to the non-AuNP-coated IDE (Figure 7), reflecting its enhanced conductivity. The incorporation of AuNPs not only improved the reproducibility of the IDE sensor but also raised the detection threshold for current, attributed to their exceptional chemical stability and biocompatibility [32]. Gold facilitates bond formation between the inorganic sensor surface and organic DNA due to its negative charges. Our findings demonstrate that the IDE sensor integrated with AuNPs produces a higher current than the uncoated sensor, aligning with the expected electrical characteristics associated with the presence of an additional layer of gold metal oxide. Overall, the I–V results validate that on-chip DNA extraction and hybridization were successful.

4. CONCLUSION

As a proof-of-concept, we demonstrated a PDMS microfluidic device for on-chip extraction and detection of *G. boninense* DNA. The AP1 buffer produced a higher DNA yield, while CTAB gave cleaner extracts. Because our biosensor relies on hybridization, the greater DNA yield from AP1 can lead to stronger signals, making AP1 preferable (though CTAB extracts have hybridized successfully). Integrating on-chip DNA extraction with a label-free interdigitated-electrode biosensor enables rapid (hour-scale) and sensitive detection of the pathogen. This approach significantly reduces sample preparation time compared to conventional PCR methods, suggesting potential for point-of-care or field diagnostics. Future work will refine buffer formulations and chip design to further improve DNA purity, yield, and sensor performance. In summary, our interdisciplinary platform demonstrates the potential of microfluidic biosensors for early Ganoderma detection in agricultural settings.

ACKNOWLEDGMENTS

Author Adilah Ayoib gratefully acknowledges support from the Institute of Nano Electronic Engineering (INEE) and the Faculty of Chemical Engineering & Technology at Universiti Malaysia Perlis (UniMAP), and the Malaysian Palm Oil Board (MPOB). Special thanks to colleagues for valuable discussions and comments. This work was supported by the NanoMalaysia Institute for Innovative Technology (NanoMite), Grant 9012 00006, funded by the Long-Term Research Grant (LRGS) from the Ministry of Education, Malaysia. The views expressed in this publication reflect the author's interpretation of the data and do not necessarily represent those of the funding agencies.

REFERENCES

[1] L. Zakaria, "Basal Stem Rot of Oil Palm: The Pathogen, Disease Incidence, and Control Methods," *Plant Dis*, vol. 107, no. 3, pp. 603–615, Mar. 2023, doi: 10.1094/PDIS-02-22-0358-FE.

[2] S. W. Dutse and N. A. Yusof, "Microfluidics-based lab-on-chip systems in DNA-based biosensing: An overview," *Sensors*, vol. 11, no. 6, pp. 5754–5768, 2011, doi: 10.3390/s110605754.

[3] A. Ayoib, U. Hashim, S. C. B. Gopinath, and M. K. Md Arshad, "DNA extraction on bio-chip: history and preeminence over conventional and solid-phase extraction methods," *Appl Microbiol Biotechnol*, vol. 101, no. 22, pp. 8077–8088, Nov. 2017, doi: 10.1007/s00253-017-8493-0.

[4] J. J. Agrestia *et al.*, "Ultrahigh-throughput screening in drop-based microfluidics for directed evolution," *Proceedings of the National Academy of Sciences*, vol. 107, no. 14, pp. 6550–6550, 2010, doi: 10.1073/pnas.1002891107.

[5] O. Mosley *et al.*, "Sample introduction interface for on-chip nucleic acid-based analysis of Helicobacter pylori from stool samples," *Lab Chip*, vol. 16, no. 11, pp. 2108–2115, 2016, doi: 10.1039/C6LC00228E.

[6] S. Julich *et al.*, "Evaluation of a microfluidic chip system for preparation of bacterial DNA from swabs, air, and surface water samples," *Biologicals*, vol. 44, no. 6, pp. 574–580, Nov. 2016, doi: 10.1016/j.biologicals.2016.06.013.

[7] N. Sandetskaya *et al.*, "An Integrated Versatile Lab-On-A-Chip Platform for the Isolation and Nucleic Acid-Based Detection of Pathogens," *Future Sci OA*, vol. 3, no. 2, May 2017, doi: 10.4155/fsoa-2016-0088.

[8] H. Wang *et al.*, "A versatile loop-mediated isothermal amplification microchip platform for Streptococcus pneumoniae and Mycoplasma pneumoniae testing at the point of care," *Biosens Bioelectron*, vol. 126, pp. 373–380, Feb. 2019, doi: 10.1016/j.bios.2018.11.011.

[9] Y. Shang, G. Xing, X. Liu, H. Lin, and J.-M. Lin, "Fully Integrated Microfluidic Biosensor with Finger Actuation for the Ultrasensitive Detection of *Escherichia coli* O157:H7," *Anal Chem*, vol. 94, no. 48, pp. 16787–16795, Dec. 2022, doi: 10.1021/acs.analchem.2c03686.

[10] A. Ayoib, U. Hashim, and S. C. B. S. C. B. Gopinath, "Automated, high-throughput DNA extraction protocol for disposable label free, microfluidics integrating DNA biosensor for oil palm pathogen, Ganoderma boninense," *Process Biochemistry*, vol. 92, no. January, pp. 447–456, May 2020, doi: 10.1016/j.procbio.2020.02.003.

[11] A. Josephin *et al.*, "Easy extraction of Ganoderma boninense liquid sample using portable on-chip device," *Indones J Biotechnol*, vol. 29, no. 1, p. 33, Mar. 2024, doi: 10.22146/ijbiotech.83645.

[12] Y.-H. Cheng, C.-H. Wang, K.-F. Hsu, and G.-B. Lee, "Integrated Microfluidic System for Cell-Free DNA Extraction from Plasma for Mutant Gene Detection and Quantification," *Anal Chem*, vol. 94, no. 10, pp. 4311–4318, Mar. 2022, doi: 10.1021/acs.analchem.1c04988.

[13] B. Xiao *et al.*, "Integrating microneedle DNA extraction to hand-held microfluidic colorimetric LAMP chip system for meat adulteration detection," *Food Chem*, vol. 411, p. 135508, Jun. 2023, doi: 10.1016/j.foodchem.2023.135508.

[14] Y. Xie *et al.*, "An open source, PCR based, point-of-care testing platform," *Sci Rep*, vol. 15, no. 1, p. 12025, Apr. 2025, doi: 10.1038/s41598-025-95639-x.

[15] L. Zhang *et al.*, "Portable DNA extraction integrated with LAMP-CRISPR/Cas12a technology for on-site detection of Salmonella Typhimurium," *NPJ Sci Food*, vol. 9, no. 1, p. 39, Mar. 2025, doi: 10.1038/s41538-025-00401-2.

[16] T. J. Saville *et al.*, "Microfluidic qPCR for detection of 21 common respiratory viruses in children with influenza-like illness," *Sci Rep*, vol. 14, no. 1, p. 28292, Nov. 2024, doi: 10.1038/s41598-024-79407-x.

[17] A. Sun *et al.*, "An integrated microfluidic platform for nucleic acid testing," *Microsyst Nanoeng*, vol. 10, no. 1, p. 66, May 2024, doi: 10.1038/s41378-024-00677-6.

[18] A. Joesaar *et al.*, "A microfluidic platform for extraction and analysis of bacterial genomic DNA," *Lab Chip*, vol. 25, no. 7, pp. 1767–1775, 2025, doi: 10.1039/D4LC00839A.

[19] C. Ianniello, J. Sero, D. Gough, B. Kasprzyk-Hordern, and N. M. Reis, "DNA extraction from bacteria using a gravity-driven microcapillary siphon," *Lab Chip*, 2025, doi: 10.1039/D4LC00735B.

[20] M. Xiong *et al.*, "Space-coded microchip for multiplexed respiratory virus detection via CRISPR-Cas12a and RPA," *Talanta*, vol. 291, p. 127815, Aug. 2025, doi: 10.1016/j.talanta.2025.127815.

[21] A. Ayoib, U. Hashim, M. K. M. K. Arshad, and V. Thivina, "Soft lithography of microfluidics channels using SU-8 mould on glass substrate for low cost fabrication," *IECBES 2016 - IEEE-EMBS Conference on Biomedical Engineering and Sciences*, pp. 226–229, 2016, doi: 10.1109/IECBES.2016.7843447.

[22] A. Ayoib, U. Hashim, S. C. B. Gopinath, V. Thivina, and M. K. M. Arshad, "Design and fabrication of PDMS microfluidics device for rapid and label-free DNA detection," *Applied Physics A*, vol. 126, no. 3, p. 193, Mar. 2020, doi: 10.1007/s00339-020-3337-7.

[23] G. Samla, K. B. Gan, and S.-M. Then, "Modeling microfluidic DNA extraction using superparamagnetic bead particles in COMSOL multiphysics simulation," *Microsystem Technologies*, pp. 1–6, 2016, doi: 10.1007/s00542-016-3170-2.

[24] J. H. Cota-Sánchez, K. Remarchuk, and K. Ubayasena, "Ready-to-use DNA extracted with a CTAB method adapted for herbarium specimens and mucilaginous plant tissue," *Plant Mol Biol Report*, vol. 24, no. 2, pp. 161–167, Jun. 2006, doi: 10.1007/BF02914055.

[25] C. G. Athanasio, J. K. Chipman, M. R. Viant, and L. Mirbahai, "Optimisation of DNA extraction from the crustacean *Daphnia*," *PeerJ*, vol. 4, p. e2004, 2016, doi: 10.7717/peerj.2004.

[26] Y. He *et al.*, "Molecular Interactions for the Curcumin-Polymer Complex with Enhanced Anti-Inflammatory Effects," *Pharmaceutics*, vol. 11, no. 9, p. 442, Sep. 2019, doi: 10.3390/pharmaceutics11090442.

[27] G. Lucena-Aguilar, A. M. Sánchez-López, C. Barberán-Aceituno, J. A. Carrillo-Ávila, J. A. López-Guerrero, and R. Aguilar-Quesada, "DNA Source Selection for Downstream Applications Based on DNA Quality Indicators Analysis," *Biopreserv Biobank*, vol. 14, no. 4, pp. 264–270, Aug. 2016, doi: 10.1089/bio.2015.0064.

[28] N. Rizan, T. Y. Shin, H. A. Tajuddin, G. Gnana kumar, and V. Periasamy, "Effect of pH on the Conductivity of Basidiomycetes DNAs Integrated Within Schottky-Like Junctions," *ChemistrySelect*, vol. 5, no. 2, pp. 601–609, Jan. 2020, doi: 10.1002/slct.201903643.

[29] G. Yammouri, H. Mohammadi, and A. Amine, "A Highly Sensitive Electrochemical Biosensor Based on Carbon Black and Gold Nanoparticles Modified Pencil Graphite Electrode for microRNA-21 Detection," *Chemistry Africa*, vol. 2, no. 2, pp. 291–300, Jun. 2019, doi: 10.1007/s42250-019-00058-x.

[30] V. Thivina *et al.*, "Distinct Detection of Ganoderma Boninense On Metal Oxides-Gold Nanoparticle Composite Deposited Interdigitated Electrode DNA sensor," *J Phys Conf Ser*, vol. 2129, no. 1, p. 012050, Dec. 2021, doi: 10.1088/1742-6596/2129/1/012050.

[31] H. Moustakim, H. Mohammadi, and A. Amine, "Electrochemical DNA Biosensor Based on Immobilization of a Non-Modified ssDNA Using Phosphoramidate-Bonding Strategy and Pencil Graphite Electrode Modified with AuNPs/CB and Self-Assembled Cysteamine Monolayer," *Sensors*, vol. 22, no. 23, p. 9420, Dec. 2022, doi: 10.3390/s22239420.

[32] A. Ayoib, "Hybrid Nanomaterials in Biosensors for Advanced Point-of-Care Diagnostics: DNA-, Enzyme-, or Immunosensor-Based, for Healthcare," in *Hybrid-Nanomaterials*, 1st ed., S. C. B. Gopinath and M. M. Ramli, Eds., Springer, Singapore, 2024, ch. 7, pp. 123–153. doi: 10.1007/978-981-97-9022-7_7.